Environ Monit Assess (2015) 187: 319
DOI 10.1007/s10661-015-4554-y

Natural radionuclide activities in forest soil horizons of Mount IDA/Kazdagi, Turkey

Özlem Karadeniz · Hidayet Karakurt · Cüneyt Akal

Received: 11 November 2014 / Accepted: 21 April 2015 / Published online: 5 May 2015

Abstract Natural radioactivity distribution of ^{40}K, ^{238}U, and ^{232}Th isotopes in forest soils was investigated by using gamma-ray spectrometry. An extensive radioecological study was carried out between 2010 and 2013 in Mount IDA/Kazdagi, located in Edremit region in Turkey. A total of 341 soil samples were collected from the surface and organic horizons (O_L, O_F+O_H, and A) in 118 soil profiles. The distributions of natural radioactivity levels in these horizons and corresponding absorbed dose rates from outdoors terrestrial gamma radiation throughout the region were mapped in detail. Mean ^{40}K activity values over the combined horizons varied between 43 and 1,008 Bq kg^{-1}; whereas, mean ^{226}Ra and ^{232}Th concentrations over the combined horizons ranged between 5–152 and 6–275 Bq kg^{-1}, respectively. Our data indicate that the radioactivity values of the study sites were within the universal normal range. The significant variation among the ^{232}Th, ^{226}Ra, and ^{40}K activities and gamma dose rate might be due to the geological variation in the study sites.

Ö. Karadeniz (✉)
Department of Physics, Faculty of Sciences, Dokuz Eylül University, 35390 Tınaztepe, İzmir, Turkey
e-mail: ozlem.karadeniz@deu.edu.tr

H. Karakurt
South-eastern Anatolian Forestry Research Institute, 23049 Elazığ, Turkey
e-mail: hkarakurt@yahoo.com

C. Akal
Department of Geological Engineering, Engineering Faculty, Dokuz Eylül University, 35390 Tınaztepe, İzmir, Turkey
e-mail: cuneyt.akal@deu.edu.tr

Keywords $^{232}Th \cdot ^{226}Ra \cdot ^{40}K \cdot$ Forest · Soil horizon · Radiological mapping

Introduction

Natural environmental radioactivity is mainly caused by the cosmic rays and from the terrestrial radiation, originated from primordial radionuclides such as ^{40}K, ^{238}U, and ^{232}Th and their decay products (UNSCEAR 2000). The external radiation exposures from these naturally occurring radionuclides contribute to nearly 20 % of the average annual dose to the human body from all radiation sources (Mohapatra et al. 2013). The level of terrestrial environmental radiations depends primarily on the geological and geographic conditions, and can be different levels in the soils of each different geological region.

Because of the complex soil properties, the forest environments can intercept and retain radionuclide deposition for a long time (Zhiyanski et al. 2008). These features produce dramatic differences in biotic concentrations of radionuclides from similar levels of deposition, and populations may be exposed to additional doses due to external irradiation or intake of radioactivity by people (Segovia et al. 2003). Therefore, forest environments are important and complex ecological systems that might have economic consequences due to possible recreational or industrial uses of the forests or their products (Gaso et al. 2000; Vaca et al. 2001).

There is now a large body of data on the activity concentrations of natural and anthropogenic

radionuclides in many areas of the world (UNSCEAR 2000) as well as many areas in Turkey. In Turkey, reported data are only related to the agricultural, rural and urban soils; granitic, volcanic, metamorphic rocks, and beach-based environment (Örgün et al. 2007; Yaprak and Aslani 2010; Canbaz et al. 2010), while the studies on forest environment are less commonly available (Karadeniz and Yaprak 2007, 2008, 2011). In addition, there are few studies on spatial analysis of natural radionuclide activity concentrations in litter (newly fallen needles/leaves), fermentation and humus layers (partly and totally decomposed material), and mineral layers, separately (Hejl et al. 2013). Especially, litter and organic layers can act as highly absorptive material for contaminants. For this reason, to assess the radiation dose delivered to humans, it is very important to obtain the present levels of natural environmental radioactivity in soil.

Therefore, a radioecological study was carried out in the forest sites of Mount IDA (Kazdagi)/Edremit. This study is the first systematic effort to provide data in this respect. We aimed to describe the spatial distribution of the ^{232}Th, ^{226}Ra, and ^{40}K isotopes in surface layers of forest soils by preparing a baseline maps of natural radionuclide activities in these forest soil horizons (O_L, O_F+O_H, and A) in the Mount IDA (Kazdagi)/Edremit. Special focus was put on the surface soil layers (O_L, O_F+O_H, and A horizons) in this study since the sources in the few inches of soil (~10 cm) account for most of the exposure rate (Beck 1972).

Materials and methods

Site descriptions

Kazdagi is located in Northwest of Asia minor, between Balikesir province and Canakkale province in Turkey (coordinates 39° 42′ N and 26° 51′ E; Fig. 1). Kazdagi has an important place in the classical mythology; its name first appears as Mount IDA in the famous epic poem "The Iliad" by Homer. Kazdagi forests have been owned and managed by the Turkish government since the foundation of modern Turkey in 1923 and the forests have been managed by the Turkish Forest Service. Some parts of the Kazdagi region became the 23rd National park of Turkey in 1993 (Uysal 2010; Kelkit et al. 2005). Since this area is one of the most important touristic, cultural, and recreational areas, it has been visited by almost million people since its establishment. Hasanboguldu and Pinarbasi forest recreational areas have been used by visitors more than 100,000 times per year (Uysal 2010; Kelkit et al. 2005; Anonymous 2002). The climate of the study area is a typical variant of mediterranean macro-climate with intensive and long summer drought seasons and irregular yearly rainfall pattern. Summers are very hot and dry (annual mean temperature is 16.4 °C), whereas winters are mild and rainy (annual mean precipitation is 664.6 mm; Uysal 2010; Kelkit et al. 2005). The precipitation occurs mainly as rainfall at the lower elevations and as snow at the higher elevations especially in winter months. Altan and Türkeş (2011) have analyzed the meteorological data for this region and concluded that the region's Thornthwaite climatic type is C_2, B'_3, s_2, b'_3, sub-humid, and mesothermal, with a severe water deficiency in the summer season. There are 355 different known plant species in Kazdagi. One third of these species have medicinal and aromatic values, and over 50 of them are endemic species. Thus, Kazdagi has been designated as a pilot genetic diversity conservation site. The conservation activity in Kazdagi conservation site has been supported by number of local, national and international projects including a World Bank GEF project.

The soil groups of Kazdagi and surrounding forests are generally lithic haploxeroll (brown forest soils), lithic xerorthent (non-calcareous brown forest soils), lithic calcixeroll (rendzina soils), typic/ calcic/ vertic rhodoxeralf (terra rosa soils) (Soil Survey Staff 2014).

The dominant forest tree species and their distribution are shown in Fig. 2. The maquis scrubland vegetation composed of leathery broadleaved Mediterranean evergreen shrubs or small trees and olive tree (*Olea europea*) orchards can be seen from the sea level to the lower slopes of the region. Calabrian pine (*Pinus brutia*, known as red pine in Turkish) is the dominant conifer species, mainly located at 200–800 m above the sea level. Crimean pine (*Pinus nigra* subsp. *pallasiana*) forests are found mainly higher elevations from 600–800 m to the alpine zone (1.400–1.600 m). There are pure and mixed oak forests composed of mainly *Quercus cerris* and *Quercus frainetto*. Other oak species like *Quercus infectoria* and *Quercus pubescens*, *Quercus ilex*, and *Quercus. coccifera* can also be found in the study area (Özel 1999; Uysal 2010). Sweet chestnut (*Castanea sativa*), beech (*Fagus orientalis*), maple (*Acer* sp.), and other temperate zone deciduous trees are found on the cool and humid slopes. Mount IDA's

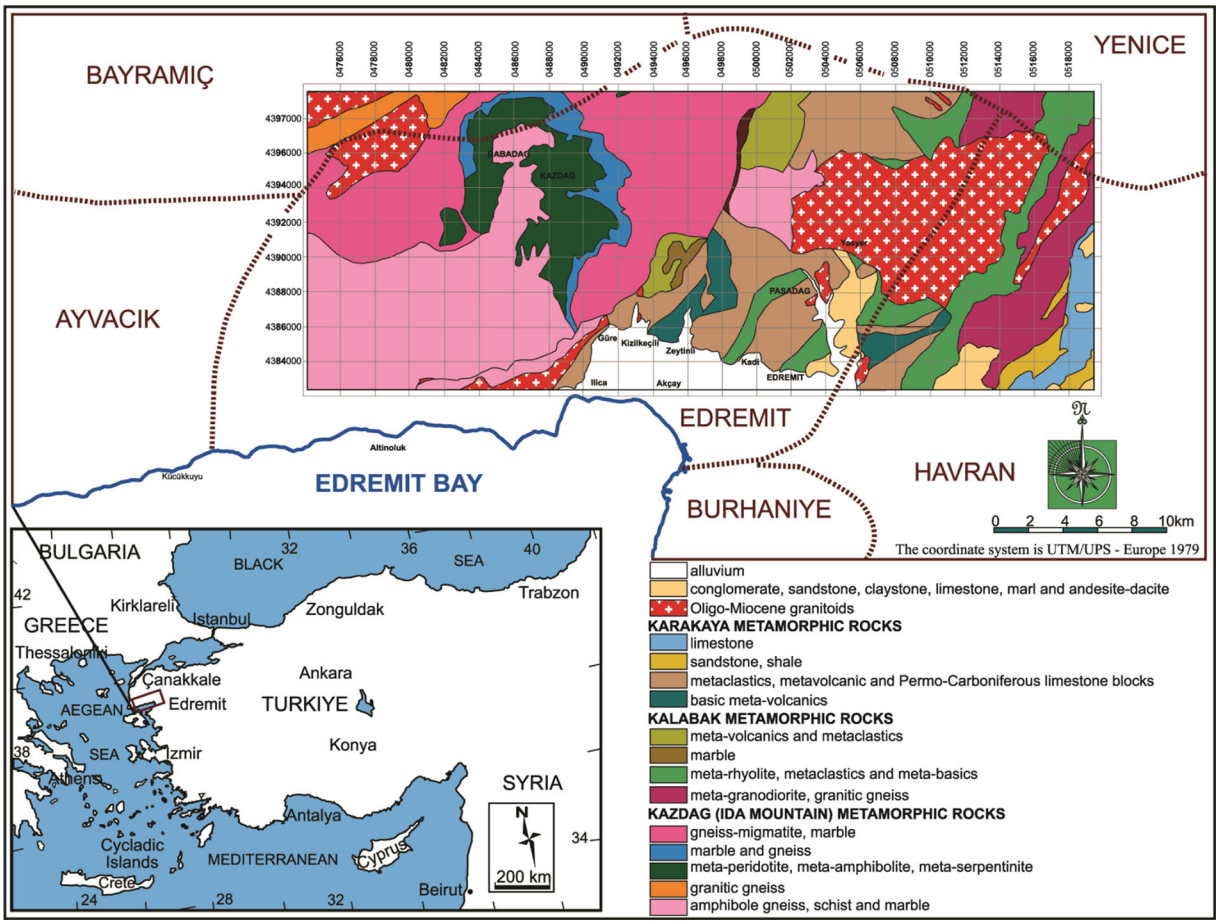

Fig. 1 Location of the study area in Ezine. The geological rock units of Kazdagi (IDA Mountain) and its surrounding area (the map is modified from Duru et al. 2007a, b

endemic species, Trojan fir (*Abies nordmanniana* subsp. *equi-trojani*) can be found on the northern humid and temperate slopes.

Geological background of Edremit Area

The detailed geological map of the area was prepared by Duru et al. (2007a, b) The rock formations of Edremit area consist of metamorphic rocks of Kazdagi, Kalabak, and Karakaya subdivisions (Fig. 1). These formations are cut by Oligo–Miocene granitoids. All of the rock formations are covered by the late Miocene sedimentary and volcanic rocks. Kazdagi metamorphics include meta-peridotites, meta-amphibolites, meta-serpentinites, amphibole gneisses, migmatites, granitic gneisses, and schist with marble. Tectonically overlying Kalabak metamorphics made up of meta-granodiorite, granitic gneisses, meta-rhyolite, meta-clastics with marble and meta-basics lenses. The general stratification of Karakaya metamorphics are represented by basic meta-volcanics, meta-volcanics and limestone block-bearing meta-clastic succession, sandstone, shale and limestone. Oligo-miocene granitoids are intruded into Kalabak and Kazdagi (Mount IDA) metamorphic rocks. Early Miocene aged andesitic–dacitic volcanic rocks and lacustrine deposits which compose of conglomerate, sandstone, claystone, limestone, marl, and andesite.

Sample collection and processing

A total of 341 soil samples were collected from 118 soil profiles between 2010 and 2013. The samples were taken from 150 rectangles of 2 km×2 km grids, covering approximately 300,000 km^2 area between the elevations of 169 and 1.485 m above the sea level. At the each sampling grid, the site characteristics such as altitude,

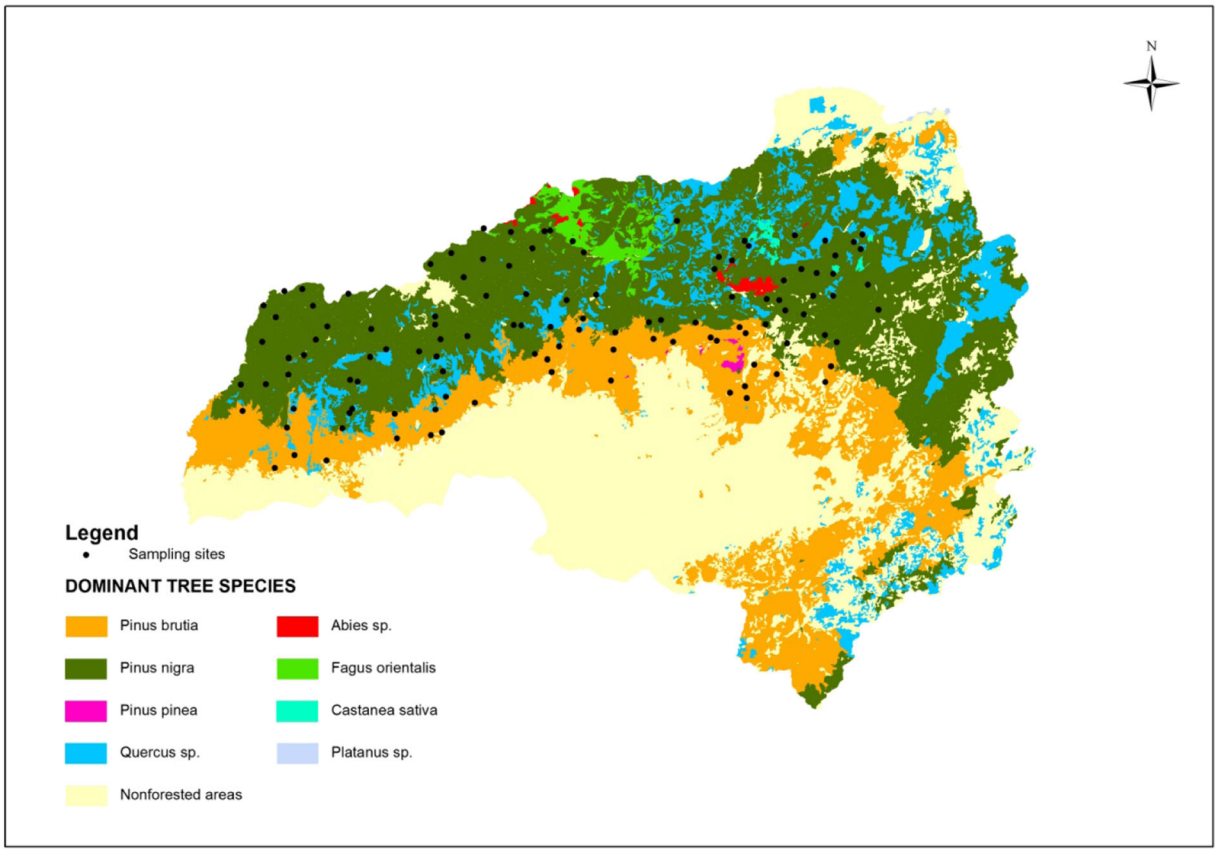

Fig. 2 Dominant forest tree species distribution map of the study area of Kazdagi

slope, exposition, forest stand description, and soil depth have been recorded. Approximately 3-kg representative sample from each forest soil layer (O_L, O_F+ O_H, and A horizons) were systematically collected. In the natural forest conditions, it was difficult to separate the O_F and O_H layers, because most of these layers had been mixed by wild animals and in some cases these are very thin to sample. The location of each sample site was determined by global positioning system, GPS Garmin Model 12XL. The soil samples were dried to a constant weight at 60 °C for 24 h in an electric oven. The mass of the samples were determined before and after the drying process. The samples were sieved using a 2-mm sieve to eliminate impurity, such as stones and roots. The mass difference after drying (d.w. loss) was calculated for each soil sample. Each dried sample (200–1,850 g) was placed in a 1.000-ml Marinelli beaker prior to analysis. The containers were sealed and stored for at least 30 days to allow secular equilibrium between ^{226}Ra, and its decay products before gamma spectroscopy measurements were made.

Gamma-spectrometric measurements

The activity concentration of ^{232}Th, ^{226}Ra, and ^{40}K in the soil samples were measured with a high resolution HPGe gamma-ray spectrometry system. The system was equipped with a coaxial p-type HPGe detector (AMETEC-ORTEC GEM40P4). The HPGe detector had a relative efficiency of 40 % with a 3"×3" cylindrical NaI(Tl) detector, an energy resolution of 1.85 at 1,332.5 keV of ^{60}Co and of 0.87 at 122 keV of ^{57}Co with a peak-to-Compton ratio of 64:1 and operating voltage of 3500 V. The detector was operated at liquid nitrogen temperature to reduce the leakage current and to increase the mobility of the charge carriers. The detector with 10-cm-thick cylindrical lead shield with low background radiation was used to shield the photons of cosmic and terrestrial origin. The detector was jacketed by a 9.5-mm-low carbon steel outer housing. The inner lining composed of 1.5-mm-thick tin layer and 1.6-mm-thick soft copper layer to prevent interference by lead X-rays. A spectroscopic amplifier

(ORTEC, Model 672), with a 16 K analog to digital converter (ASPEC-927) used to process the signals. The MAESTRO-32 multichannel analyzer emulation software was used for peak searching, peak evaluation, energy calculation, nuclide identification, data acquisition, storage, display, and on-line analysis of the spectra.

The energy calibration was obtained using standard sources from SPECTECH: ^{60}Co and ^{152}Eu for an energy range between 120 and 1,400 keV and analyzed in the same conditions. The IAEA reference materials RGU-1 (U-ore), RGTh-1 (Th-ore), and the potassium standard was prepared from pure potassium chloride with similar densities for absolute efficiency calibration of the gamma spectrometry system. The reference standard sources were prepared in Marinelli beakers to have the same counting geometry of the samples. For the reliability of counting efficiency, additional quality control checks were carried out using the IAEA-375 reference material of known activities (424 Bq kg^{-1}of ^{40}K, 20 Bq kg^{-1} of ^{226}Ra, and 20.5 Bq kg^{-1} of ^{232}Th). The activities of this sample were in accordance with its certified values within 5 % error margin.

The sample containers were placed on detector endcap for counting. The accumulating time of the sample spectra was ranged between 10,000 and 20,000 s to obtain a gamma spectrum with good statistics. To determine the background distribution due to naturally occurring radionuclides in the environment around the detector, an empty Marinelli beaker with a volume of 1,000 ml with the same geometry was used. This background measurement which was taken during one weekend (200,000 s) was subtracted from the sample measurements to correct the net peak area of gamma rays of the measured isotopes.

The activity concentration of ^{226}Ra was derived from the weighted average of the activities of the three gamma-ray line of 609.3, 1,120.3, and 1,764.5 keV from ^{214}Bi and of one gamma-ray line of 351.9 keV from ^{214}Pb, while the gamma-ray lines of the 911.2 keV from ^{228}Ac, the 727.3 keV from ^{212}Bi, and 583.2 and 2614.5 keV from ^{208}Tl were used to determine the activity concentration of ^{232}Th. Several peaks from ^{226}Ra and ^{232}Th daughters were also monitored. The activity concentration of ^{40}K was obtained using its 1461 keV gamma-ray line. The statistical errors were considered only for the counting statistical uncertainty, which were found in the order of 1–3 % for high activities and more than 10 % for the small activities at the 95 % level of confidence. The minimum detectable activity (MDA) based on Currie (1968) for the counting time of 20,000 s was 0.17 Bq kg^{-1} for ^{214}Pb (351 keV); 0.22 and 0.59 Bq kg^{-1} for ^{208}Tl (583 and 2,614 keV); 0.21, 0.47, and 0.59 Bq kg^{-1} for ^{214}Bi (609, 1,120, and 1,764 keV); 0.17 Bq kg^{-1} for ^{228}Ac (911 keV); 0.41 Bq kg^{-1} for ^{212}Bi (727.3 keV); and 1.15 Bq kg^{-1} for ^{40}K (1,460 keV).

Statistical analysis

All statistical evaluations were carried out with SPSS 13.0 version. Statistical analyses for possible significant correlations between the parameters were performed with using linear regression analysis. The Kolmogorov–Smirnov test (significance level $p>0.05$) was used to test the frequency distribution of data sets against a normal or lognormal distribution.

Results and discussion

The use of gamma-ray spectrometry for quantitative mapping of surface radioelement distribution was established during the late 1960s. Because of their almost ubiquitous distribution and sensitivity as indicators of geological processes, the naturally occurring radioelements are of considerable geochemical significance. Spatial radioelement patterns can be used to distinguish the rock formation patterns. These patterns can be used to determine the areas of potential mineralization (IGCP Project 259). The distributions of the naturally occurring radionuclides show a significant variation due the variation in the geological structure of the sites. Thus, the distributions of ^{232}Th, ^{226}Ra, and ^{40}K activities in forest soil horizons (O_L, O_F+O_H, and A) and the average activities (Bq kg^{-1}) over the combined horizons throughout the region were mapped in detail.

Contour map of the ^{232}Th, ^{226}Ra, and ^{40}K activity concentrations was created with ordinary Kriging interpolation method. A variogram of the data were calculated in order to obtain the correlation of the data as a function of the distance. The variations across the unsampled sites were also taken into consideration (Aslani et al. 2003; Khoshbinfar and Moghaddam 2012). All these geostatistical analyses have been carried out using version 9 of SURFER software. Spatial distribution patterns of ^{232}Th, ^{226}Ra, and ^{40}K activities in forest soils throughout the region were estimated and

the results are shown in Figs. 3, 4, and 5 as a contour map.

For a more general and representative overview, summary statistics for the activity concentration of ^{40}K, ^{226}Ra, and ^{232}Th in forest soil horizons collected from Mount IDA are given in Table 1. In Table 1, description of soil profiles was given and meaning of each (sub-) horizons was presented: O_L—newly fallen litter consisting sub-horizon; O_F+O_H—partly and totally decomposed litter consisting sub-horizon; A—topsoil horizon. Based on 118 collected soil profiles, activity concentrations of ^{232}Th in O_L horizons varied between 0.4–40 Bq kg^{-1} (dry wt.) with a geometric mean of 3.4 Bq kg^{-1} (dry wt.). The ^{232}Th activity concentrations in O_F+O_H and A horizons were 2.5–203 Bq kg^{-1} with a geometric mean of 34 Bq kg^{-1} (dry wt.) and 5.5–290 Bq kg^{-1} (dry wt.) with a geometric mean of 48 Bq kg^{-1} (dry wt.), respectively. The ^{226}Ra activity concentration in O_L horizons varied from 0.5 to 26 Bq kg^{-1} with a geometric mean of 3.3 Bq kg^{-1}. The ^{226}Ra concentrations in O_F+O_H and A horizons were 3.5–121 Bq kg^{-1} with a geometric mean of 27 and 5.5–156 Bq kg^{-1} with a geometric mean of 36 Bq kg^{-1}, respectively. Activity concentrations of ^{40}K in O_L horizons varied between 7 and 452 Bq kg^{-1} with a geometric mean of 73 Bq kg^{-1}, while the ranges of ^{40}K concentrations in O_F+O_H and A horizons were 90–765 Bq kg^{-1} with a mean of 398 and 94–1,118 Bq kg^{-1} with a mean of 570 Bq kg^{-1}, respectively (Table 1).

The Kruskal–Wallis test which was used to evaluate the differences between the mean values of ^{232}Th, ^{226}Ra, and ^{40}K activity concentrations obtained for O_L, O_F+O_H, and A horizons. Test results (mean rank, standard deviation, chi-square value, and p values) are provided in Table 2. Statistical analysis showed that there was a statistically significant difference in these radionuclide activity levels between the O_L, O_F+O_H, and A horizons. Namely, mean rank activity concentrations of ^{232}Th, ^{226}Ra, and ^{40}K for A horizons were significantly higher than that of O_L and O_F+O_H horizons ($p<0.05$).

The upper forest soil layers often have a large undecomposed organic component, which consisted of leaf litter, animal residues, needles, twigs, branches, and fruits (i.e., seeds, acorns, cones, etc.). The fermentation and humus layers (O_F and O_H) under the upper layer, made of partly and fully decomposed organic matter, giving the soil distinct dark color compared to the lower mineral soil horizons (i.e., A horizon). As we go down the soil profile, loose and partly decayed organic content of the layer is replaced with the mineral matter mixed with some humus. Some of the cations like potassium (K), thorium (Th), and radium (Ra) can be more abundant in the lower layers because of the bedrock contents of these forest sites. Soil micro- and macro-fauna, from earthworms to wild boars, mix the soil organic layers and topsoil (A horizon) to get food such as bulbs and truffles, which might explain some of the upward movement of the radioactive material. Since the litter layer as a topmost soil horizon is made of undecomposed organic matter and is not mixed with the mineral matter, the natural radioactivity levels of the litter, fermentation, and humus layers of these forest soils are lower than the other layers (Figs. 3, 4, and 5).

Figure 6 shows the correlation between the specific activities of ^{40}K, ^{226}Ra, and ^{232}Th isotopes in the samples taken from the A—topsoil horizons. There was a significant correlation among the concentrations of the $^{232}Th/^{226}Ra$ ($R^2=0.819$), $^{40}K/^{226}Ra$ ($R^2=0.570$), and $^{40}K/^{232}Th$ ($R^2=0.503$) in the soil samples. These results are in agreement with the findings of some previous studies (Öztürk et al. 2013; Karadeniz and Akal 2014).

The level of terrestrial environmental radiation in an area is affected by the geological composition of the area. The thorium (Th), uranium (U), and potassium (K) content of the parent rocks also has a significant effect on the radiation emitted by the soils (Tzortzis and Tsertos 2004). The analysis of the NORM relative abundance (Th/U, K/U, and K/Th ratios) may also give information on the relative enrichment/depletion processes as a result of the complex metamorphic history of the rocks. In addition, these patterns can be used to indicate the areas of potential mineralization, which are not restricted to U and Th minerals (Verdoya et al. 2001; Chiozzi et al. 2002; Alnour et al. 2012). As followed in Fig. 7, which includes all measurements of ^{232}Th and ^{226}Ra for the investigated area, the oligo-miocene granitoids have the highest contents of ^{232}Th and ^{226}Ra. It is followed by meta-granite and gneisses. The lowest values of ^{232}Th and ^{226}Ra belong to amphibole gneiss, schist, and marble group and meta-volcanic and metaclastic group and meta-rhyolite, metaclastics, and meta-basics (see Fig. 1). The moderate values measured from gneiss-migmatite, marble group and metaclastics, meta-volcanic, and permo-carboniferous limestone blocks group. The classification on this binary diagram can also see in Figs. 3, 4, and 5 belong to the anomaly maps of soil horizons.

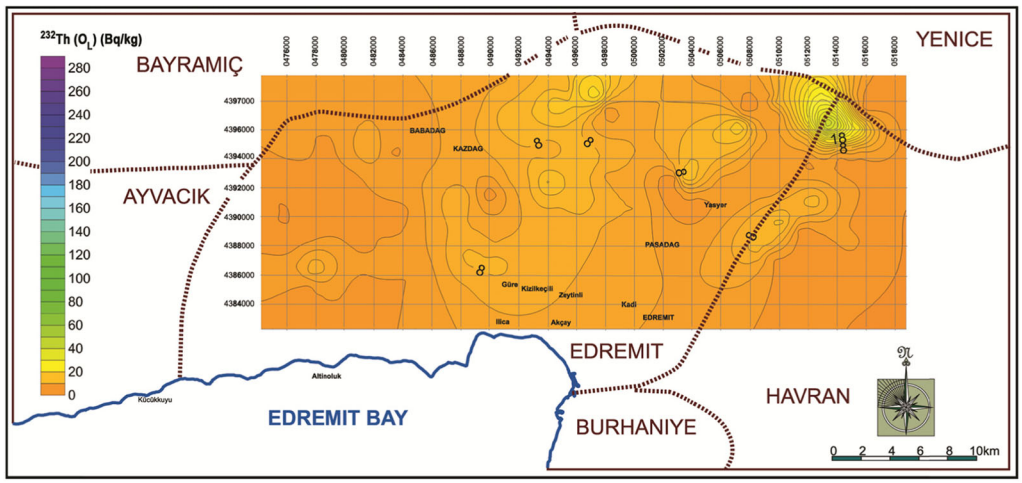

(a)

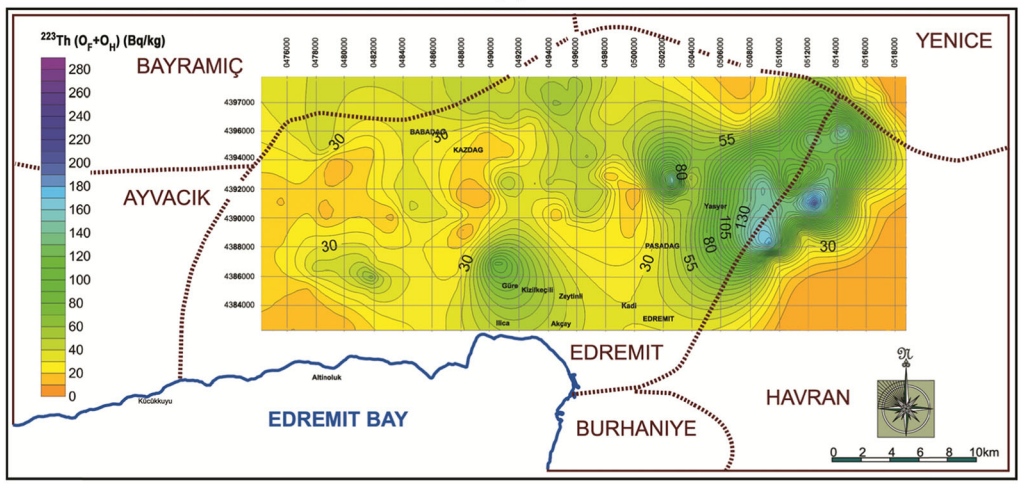

(b)

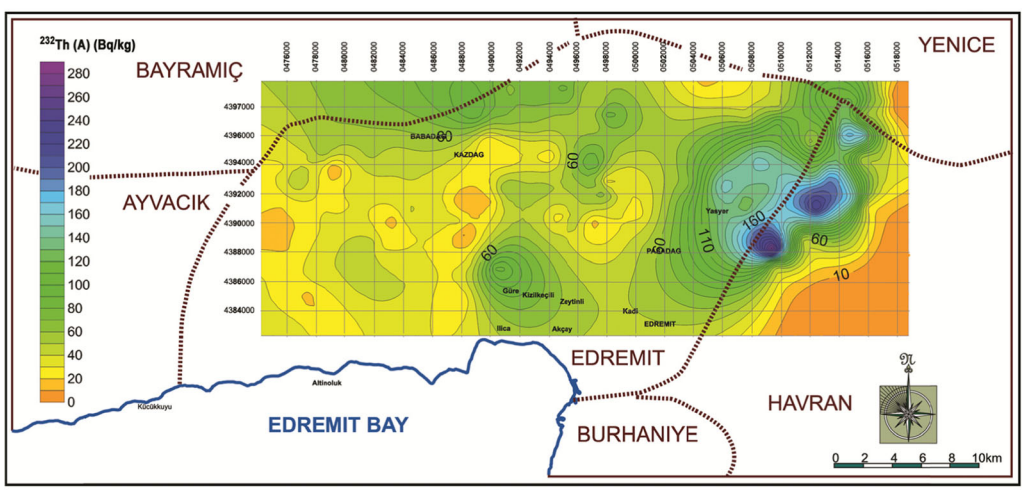

(c)

Fig. 3 Interpolated radiological maps of ^{232}Th activity concentration in **a** O_L, **b** O_F+O_H, and **c** A soil horizons collected from Mount IDA (Kazdagi)/Edremit

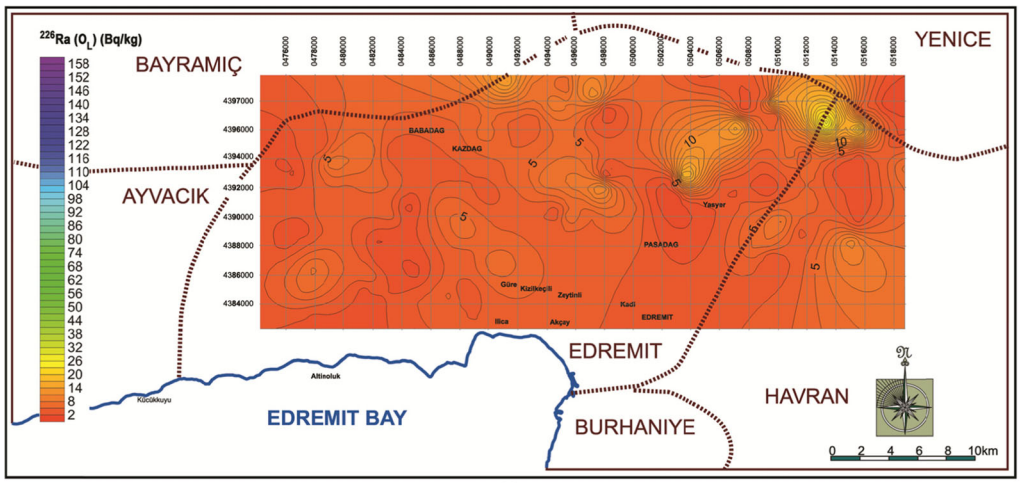

(a)

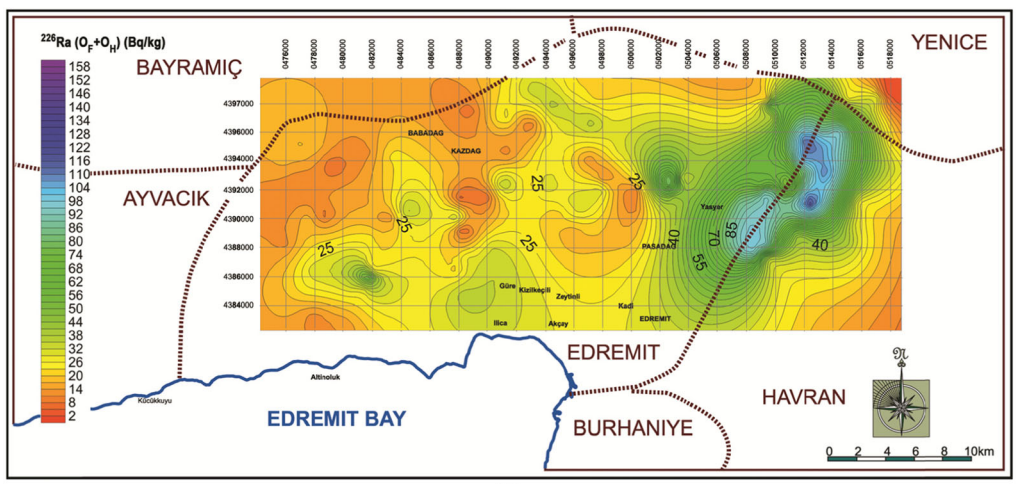

(b)

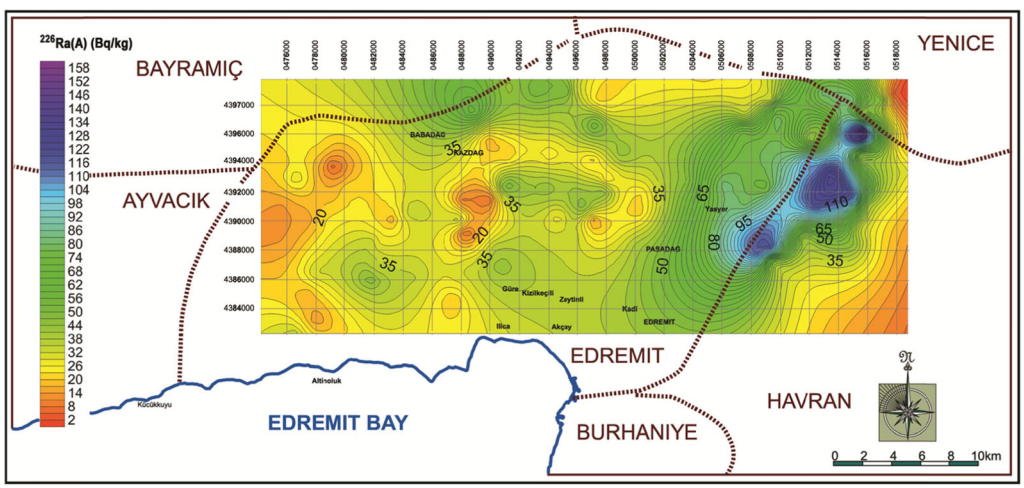

(c)

Fig. 4 Interpolated radiological maps of ^{226}Ra activity concentration in **a** O_L, **b** O_F+O_H, and **c** A soil horizons collected from Mount IDA (Kazdağı)/Edremit

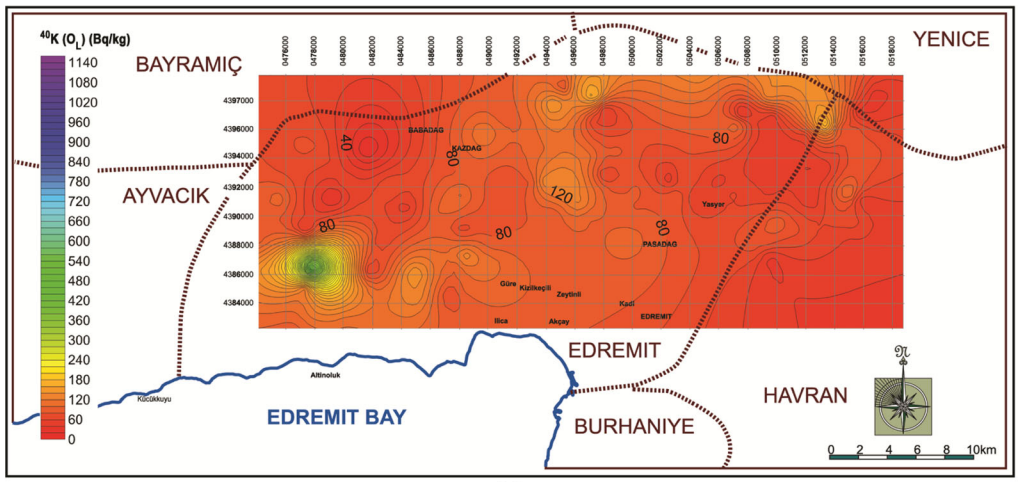

(a)

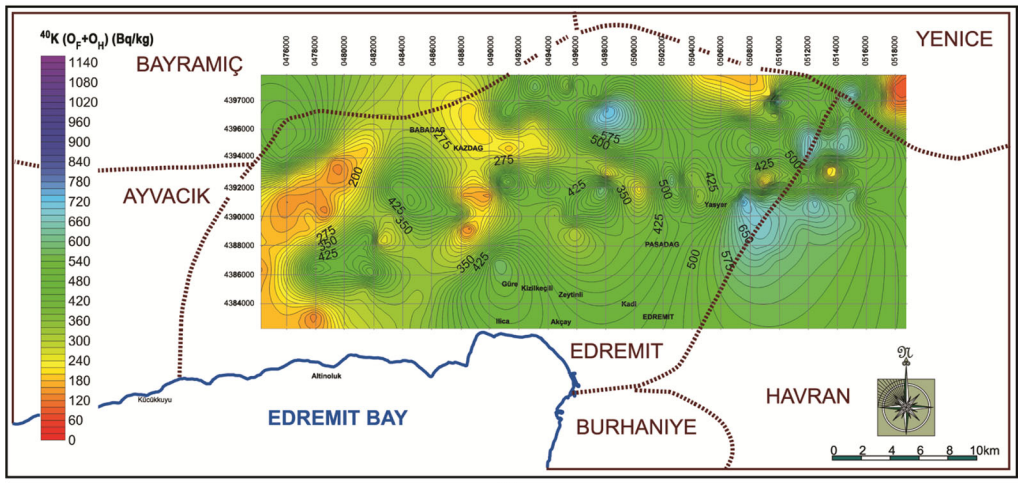

(b)

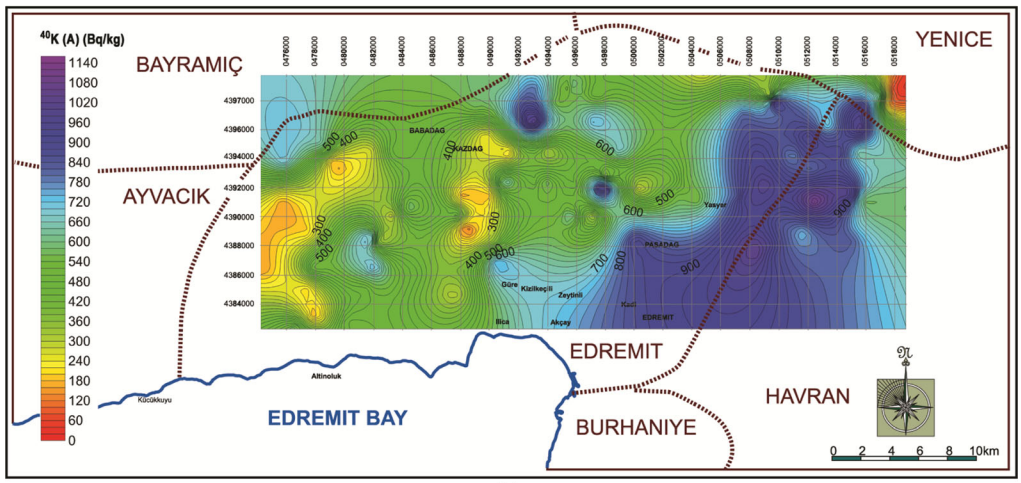

(c)

Fig. 5 Interpolated radiological maps of ^{40}K activity concentration in **a** O_L, **b** O_F+O_H, and **c** A soil horizons collected from Mount IDA (Kazdağı)/Edremit

Table 1 Summary statistics for the activity concentration of ^{232}Th, ^{226}Ra, and ^{40}K for soil horizons (O_L, O_F+O_H, and A) and activity concentrations averaged over the combined horizons (Bq kg^{-1}) of Mount IDA

	O_L (Bq kg^{-1})	O_F+O_H (Bq kg^{-1})	A (Bq kg^{-1})	Average activity (Bq kg^{-1})
^{232}Th				
Median	3.51	32	47	43
Mean±S.E.	5.36±0.53	47±4	64±5	59±4
S.D.	5.98	41	52	48
GM	3.39	34	48	45
CV (%)	107	87	81	81
GCV (%)	169	120	108	107
Range	0.44–40	2.53–203	5.50–290	6–275
Skewness	2.94	1.75	1.69	1.79
Kurtosis	13.2	2.56	3.15	3.67
Frequency distribution	Log-normal	Log-normal	Log-normal	Log-normal
^{226}Ra				
Median	3.58	26	36	33
Mean±S.E.	4.55±0.38	35±3	45±3	42±3
S.D.	4.09	27	31	30
GM	3.29	27	36	33
CV (%)	90	78	68	71
GCV (%)	124	101	85	89
Range	0.5–26	3.5–121	5.50–156	5–152
Skewness	2.47	1.50	1.40	1.47
Kurtosis	8.03	1.45	1.53	1.77
Frequency distribution	Log-normal	Log-normal	Log-normal	Log-normal
^{40}K				
Median	77.5	398	570	509
Mean±S.E.	91.9±4.30	398±17	570±24	516±23
S.D.	46.7	178	264	246
GM	73	351	498	442
CV (%)	57	45	46	48
GCV (%)	64	51	53	56
Range	7–452	90–765	94–1118	43–1008
Skewness	4.40	0.08	0.08	0.04
Kurtosis	32.9	−1.02	−0.96	−1.00
Frequency distribution	Log-normal	Normal	Normal	Normal

Median, mean (arithmetic mean), standard error of arithmetic mean (S.E.), standard deviation (S.D.), geometric mean (GM), coefficient of variation (CV), geometric coefficient of variation (GCV), range, expressed in Bq kg^{-1} and skewness, and kurtosis of the frequency distributions of ^{137}Cs activities

The radiological anomaly maps of O_F+O_H and A horizons indicates highest anomalies of ^{232}Th, ^{226}Ra, and ^{40}K which related with tick of arenitic granitoid soil layers on granitoidic part of geological map (Fig. 1). The ^{226}Ra and ^{232}Th activities of soil samples are high because of concentration of heavy minerals such as sphene and zircon crystals in granitoid arenitic soil. The highest ^{40}K anomalies on granitoidic part of the maps are related with presence of biotite and amphibole crystals derived from granitoid and meta-granitoid of Kazdağ region.

As shown Figs. 3, 4, and 5, the regional distributions and the depositions of the natural radionuclides (^{232}Th, ^{226}Ra, and ^{40}K) in the soils are affected by the underlying geological processes. The soil samples which are taken from oligo-miocene granitoids and meta-granitoid and granitic gneisses present high variations in radioactivity. The Ra and Th anomalies can be attributed to the

Table 2 Kruskal–Wallis test table for ^{232}Th, ^{226}Ra, and ^{40}K

Horizon	N[a]	Mean rank	SD[b]	χ^{2}[c]	p[d]
^{232}Th					
O_L	118	64.35	2	220,366	0.0001
O_F+O_H	113	214.99			
A	118	247.35			
^{226}Ra					
O_L	118	63.79	2	222,520	0.0001
O_F+O_H	113	215.31			
A	118	247.61			
^{40}K					
O_L	118	62.34	2	233,766	0.0001
O_F+O_H	113	209.58			
A	118	254.55			

[a] Cases

[b] Standard deviation

[c] Chi-square value

[d] p value<0.05 is significant

presence of rare earth elements in the heavy minerals such as sphene, zircon, and monazite in soil samples. The ^{40}K isotope activity show high variation, especially on oligo-miocene granitoids, meta-granitoid, granitic gneisses, migmatites, and schists (Fig. 5). The common mineralogical composition of these rocks consists of orthoclase, plagioclase, biotite, and amphibole which are potassium-rich minerals and generally produce clay mineral related to alteration. These potassium-bearing and altered minerals can cause high ^{40}K anomalies in the region.

In order to derive the average activities over the combined horizons, the densities of the three layers were taken into account. The mean activity concentrations measured for the O_L, O_F+O_H, and A horizons were weighted with the corresponding area-related density as indicated by Rühm et al. (1999). The resulting ^{40}K activity concentrations averaged over the depth sections varied within the limits from 43 to 1,008 Bq kg^{-1} with a mean of 516 Bq kg^{-1}, while the ranges of ^{226}Ra and ^{232}Th concentrations were 5–152 Bq kg^{-1} with a

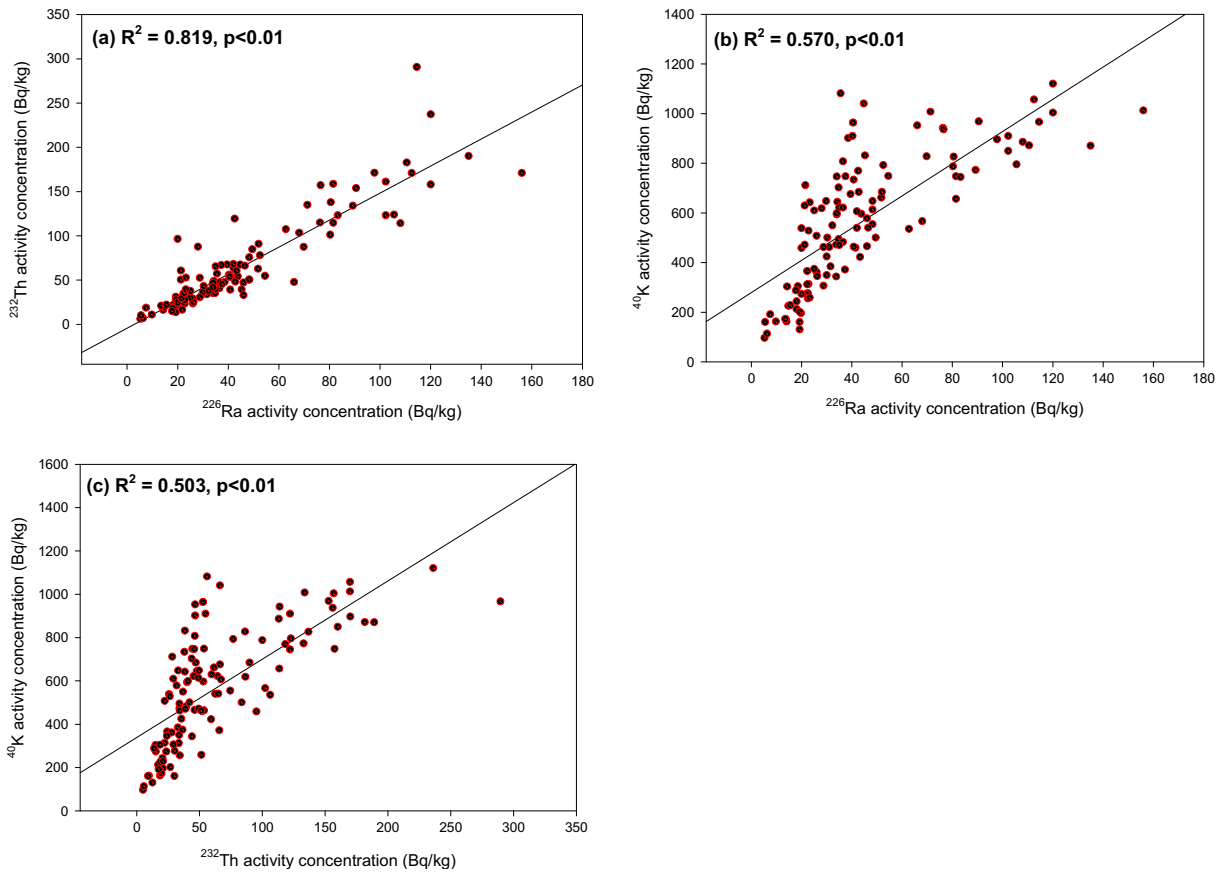

Fig. 6 Scatter plot of A—topsoil horizon ^{226}Ra versus ^{232}Th (**a**), ^{226}Ra versus ^{40}K (**b**), and ^{232}Th versus ^{40}K (**c**) with linear regression lines

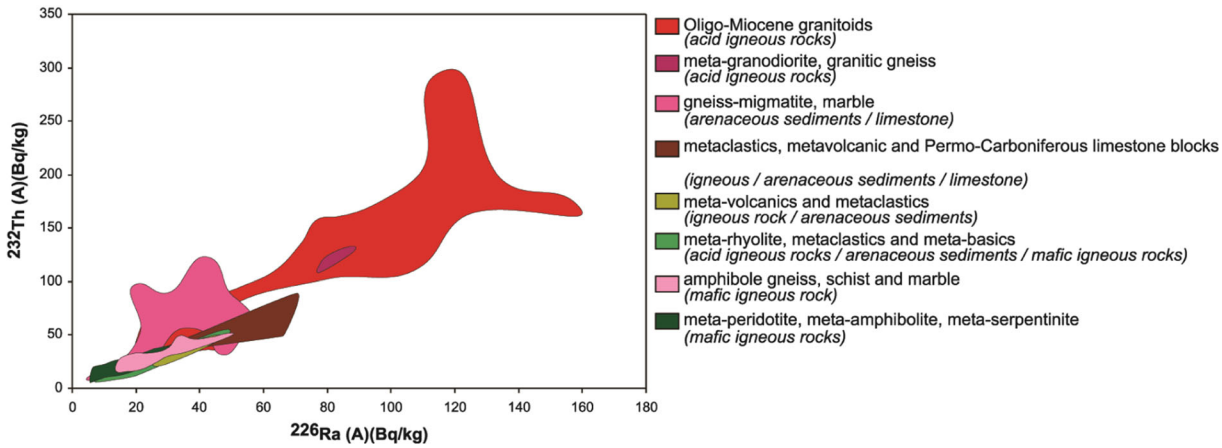

Fig. 7 ^{232}Th (Bg/kg) versus ^{226}Ra (Bq/kg) contents of A—topsoil horizon samples together with classification scheme of Clark et al. (1966) around Kazdagi (Mount IDA) region (The litologies are in Fig. 1)

geometric mean of 33 and 6–275 Bq kg^{-1} with a geometric mean of 45 Bq kg^{-1}, respectively. It is important to note that the estimations on all mean concentrations of ^{226}Ra, ^{232}Th, and ^{40}K in soil in areas of normal radioactivity given in the recent UNSCEAR 2000 report are 35, 30, and 400 Bq kg^{-1}, respectively, and typical ranges are 17–60 Bq kg^{-1} for ^{226}Ra, 11–64 Bq kg^{-1} for ^{232}Th, and 140–850 Bq kg^{-1} for ^{40}K. In the light of the above knowledge, the values obtained fall within the typical range of worldwide average values.

As mentioned above, ^{238}U and ^{232}Th series nuclides and ^{40}K in soil are arised mainly from underlying bedrock. Environmental conditions such as weathering, sedimentation, leaching, and precipitation from percolating ground water or dilution with other materials with different composition influence the distribution of these radionuclides. It is reported that as a plant uptake radionuclide ^{40}K in soils varies with soil pH, depending on the plant species, while the distribution of uranium concentrations are related to soil organic matter content (Fujiyoshi and Sawamura 2004 and further references cited therein). Therefore, their activity concentrations and their gradients with depth varied from one location to another (Figs. 3, 4, and 5).

The shape of the frequency distributions of the ^{40}K, ^{226}Ra, and ^{232}Th activity concentration; the mass concentration averaged over the soil column was studied. The measured histograms were compared with the normal and log-normal distribution functions using Kolmogorov–Smirnov test values for the goodness-of-fit (Karadeniz and Yaprak 2007). Accordingly, the values of the coefficients of skewness and kurtosis, and the type of the frequency distributions were also summarised in Table 1. Application of the Kolmogorov–Smirnov test and the approximate null value of the skewness coefficient obtained for ^{40}K activities of soils show that this distribution is practically symmetrical, while the positive values obtained in the statistics of other natural radionuclide activities in soil samples indicate that the distribution is asymmetric (Fig. 8). Because the results fit to a log-normal distribution fairly well, it is convenient to use the geometric mean values as a mean rather than arithmetic mean (Öztürk et al. 2013).

The dose rates at 1 m above the ground level resulting from the gamma emitting radionuclides in the ^{40}K, ^{226}Ra and ^{232}Th for uniform distribution in soil profile were calculated from concentrations of these radionuclides using the following equation (UNSCEAR 2000):

$$D\left(\text{nGy h}^{-1}\right) = 0.0417\,C_K + 0.462\,C_{Ra} + 0.604\,C_{Th} \quad (1)$$

where D is the dose rate in air outdoors, C_K, C_{Ra}, and C_{Th} the activity concentrations of ^{40}K, ^{226}Ra, and ^{232}Th in the soil sample, respectively. During calculation, secular equilibrium was assumed to exist between radionuclides and their progeny within each series.

Interpolated radiological maps of the outdoor absorbed dose rate in air outdoors just from the terrestrial radionuclides in soils for Mount IDA (Kazdağı)/Edremit are shown in Fig. 9 as a

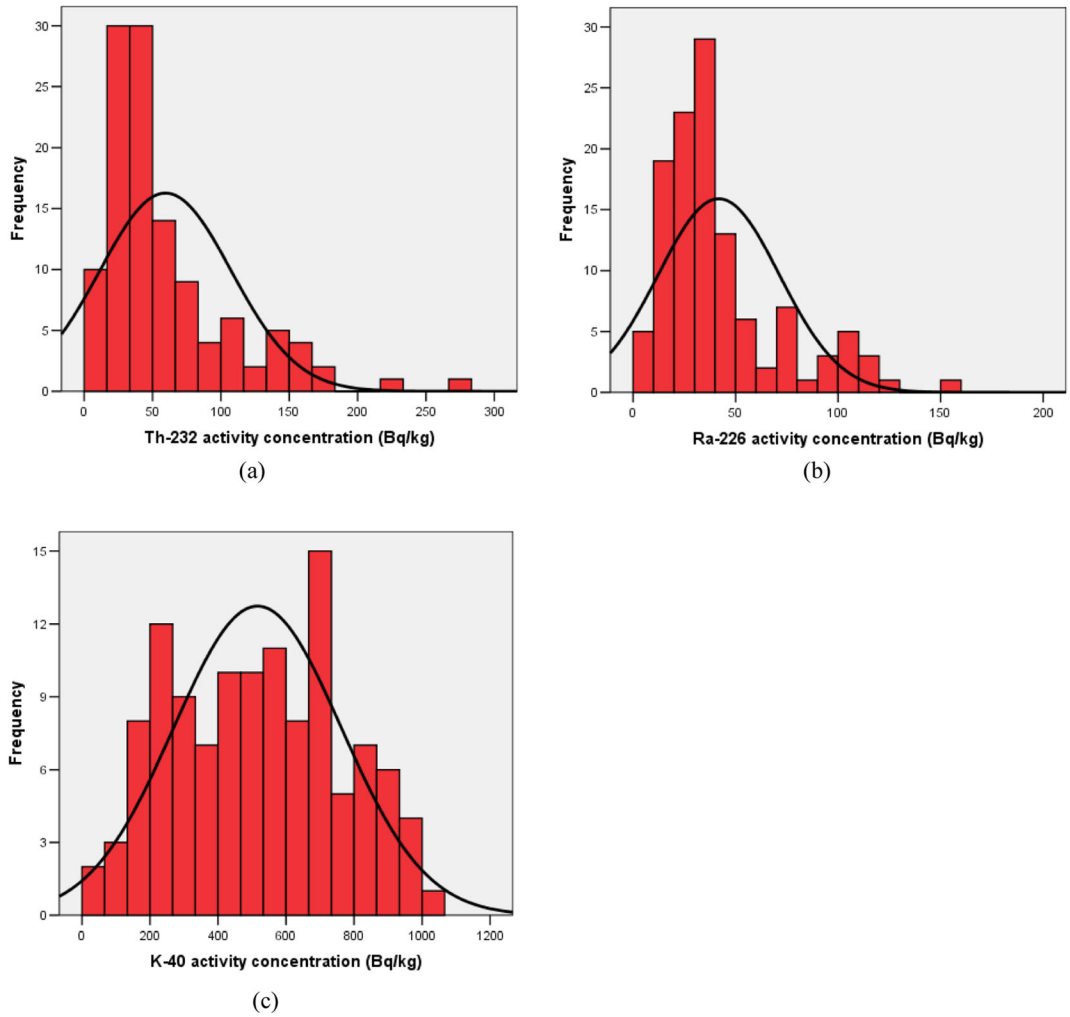

Fig. 8 Frequency distributions of **a** ^{232}Th, **b** ^{226}Ra, and **c** ^{40}K concentration (Bq kg^{-1}). Also shown are fits of the ^{232}Th, ^{226}Ra concentration to a log-normal distribution, and the ^{40}K concentration to a normal distribution

contour map. The outdoor absorbed dose rate ranged between 10 and 256 nGy h^{-1} with a mean of 77 nGy h^{-1} and was found to be within the typical range of worldwide average values (10–200; UNSCEAR 2000). The contribution to the total absorbed gamma dose rate in the air in the decreasing order was due to the presence of ^{232}Th (44 %), followed by ^{40}K (31 %) and ^{226}Ra (25 %) in soil samples (Fig. 10).

In the UNSCEAR 2000 Report, a coefficient of 0.7 Sv Gy^{-1} was used to convert absorbed dose in the air to the effective dose equivalent for environmental exposures to gamma rays of moderate energy. If the outdoor occupancy factor to be 0.2, the annual effective dose equivalent from outdoors in units of μSv is calculated by the following formula:

$$\text{Effective dose rate } (\mu\text{Sv a}^{-1}) = \text{Dose rate } (\text{nGy h}^{-1}) \times 8760\ (\text{h a}^{-1}) \times 0.2\ (\text{occupancy factor}) \times 0.7\ \text{Sv Gy}^{-1}\ (\text{conversion coefficient}) \times 10^{-3} \quad (2)$$

In this regard, the annual effective dose from external exposure to terrestrial radionuclides in the surveyed area ranging from 12 to 314 μSv year^{-1} with a mean value of 94 μSv year^{-1} for soils.

The gamma-ray radiation hazards due to the specified radionuclides were assessed by currently used indices as radium-equivalent activity (Ra_{eq}) and external radiation

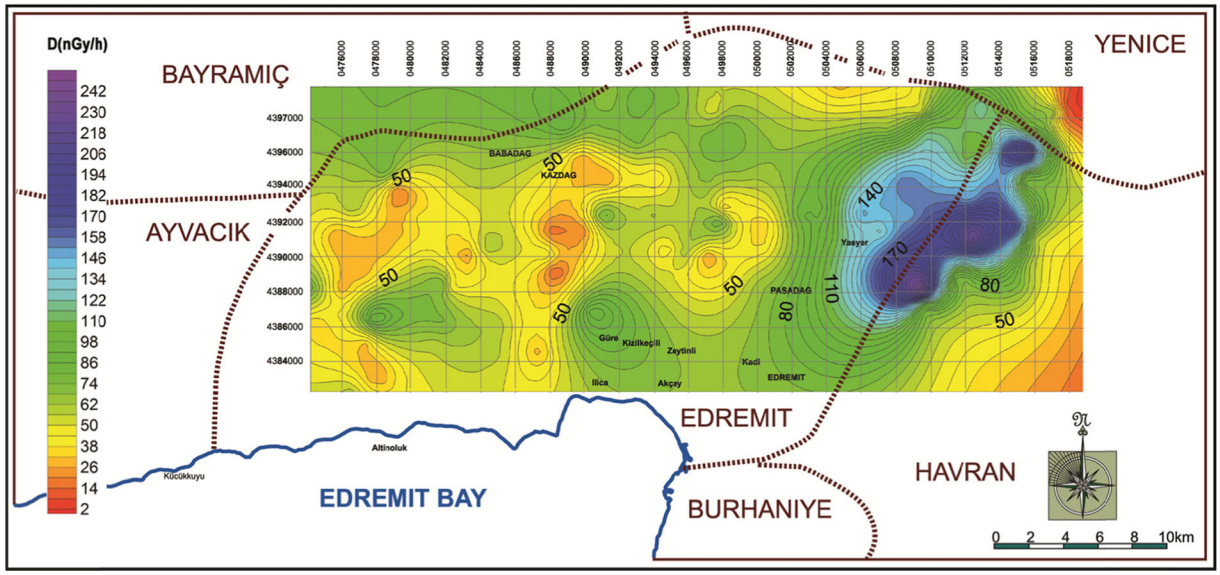

Fig. 9 Interpolated radiological maps of the outdoor absorbed dose rate in air outdoors just from the terrestrial radionuclides in soils for Mount IDA (Kazdağı)/Edremit

hazard (H_{ex}). The Ra_{eq} of a sample is given by (Beretka and Mathew 1985; Krieger 1981):

$$Ra_{eq} = 0.077\,C_K + C_{Ra} + 1.43C_{Th} \quad (3)$$

where C_K, C_{Ra}, and C_{Th} and are the average activity concentrations of ^{40}K, ^{226}Ra, and ^{232}Th, in Bq kg^{-1}, respectively. Estimated Ra_{eq} values for the collected samples varied from 22 to 575 Bq kg^{-1}, and some values are higher than the recommended maximum value of 370 Bq kg^{-1} (Beretka and Mathew 1985; OECD 1979).

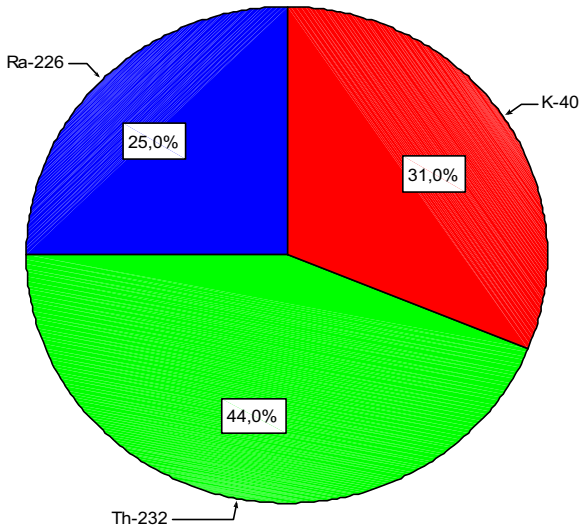

Fig. 10 The contribution of ^{40}K, ^{226}Ra, and ^{232}Th to the total absorbed gamma dose rate in air

To limit the annual external gamma-ray dose (UNSCEAR 1982) to 1.5 mGy for the samples under investigation, the external hazard index (H_{ex}) is given by the following equation:

$$H_{ex} = C_K/4810 + C_{Ra}/370 + C_{Th}/259 \leq 1, \quad (4)$$

The results of H_{ex} based on the criterion formula (Eq. 4) range from 0.06 to 1.58.

The gamma index ($I\gamma$) proposed by the European Commission (1999) is defined in order to assess gamma-ray radiation originating from building materials. This index can be expressed as;

$$I\gamma = \frac{C_{Ra}}{300} + \frac{C_{Th}}{200} + \frac{C_K}{3000} \quad (5)$$

where, C_{Ra}, C_{Th}, and C_K are the specific activities of ^{226}Ra, ^{232}Th, and ^{40}K isotopes, respectively. The values 300, 200, and 30,00 Bq kg^{-1} were calculated for a dose criteria limit of 1 mSv year^{-1}. Based on this criterion, $I\gamma$ is ranged from 0.08 to 2.05 and $I\gamma$ values are less than unity in most of samples.

Conclusion

Gamma-radiation from naturally occurring radionuclides and from radionuclide deposited on the ground is the main external source of irradiation of the human body. Studies of terrestrial natural radiation are of great

importance for several reasons. Firstly, most of the radioactivity in the terrestrial environment is bound to the components of the soils. Transportation of this radioactivity from soil is possible to vegetation via dust deposition or root uptake, water sources by flood washdown, and forward to humans through inhalation (Ramli 1997). Determining the distribution of terrestrial radionuclides that originate from soil is potentially important for radiation risk assessment and performing epidemiological studies. Secondly, they serve as baseline data of natural radioactivity in order to ascertain possible changes in environmental radioactivity due to nuclear, industrial, and other human activities (Tufail et al. 2006). The results obtained in each country can be exploited to enrich the world's data bank, which is importantly needed for evaluating worldwide average values of radiometric and dosimetric quantities, in addition to guide decision-markers in solving some natural environmental problems which may be found anywhere in the world (Jamal Al-Jundi 2002; Tzortzis et al. 2003). Therefore, investigations on terrestrial natural radiation have received particular attention worldwide and let to extensive surveys in many countries.

The forest environment is an important and complex ecological system with great capacity to intercept and to retain radionuclide deposition for a long time (Zhiyanski et al. 2008). Both the natural and the man-made isotopes present in forests can perturb the evolution of ecosystems since the soil properties of those ecosystems produce dramatic differences in biotic concentrations of radionuclides from similar levels of deposition (Segovia et al. 2003). This is very important environmental facts which have many effects, determining the intake of radioactivity by people, including economic consequences, due to the possible recreational or industrial uses of the forest or its products (Gaso et al. 2000; Vaca et al. 2001). For this reason, the knowledge about the radionuclides behavior in forest ecosystems has a very important ecological role for better understanding of element fluxes, balances, and dynamics, and such studies have been receiving much attention during the recent years (Ylipieti et al. 2008; Nada et al. 2009). Litter and organic layers can act as highly absorptive material for contaminants in forest ecosystem. Plant roots, as well as the hyphae of their associated mycorrhizal associations (e.g., mushroom fruiting bodies), are also mainly located in humus layer where soil to plant transfer occurred. Therefore, concentrations in the humus layer reflect the levels of radioactive contamination and provide important information when assessing the current state of the environment.

Mount IDA/Kazdagi is one of the most important touristic, cultural, and recreational areas; it has been used by visitors more than 100,000 times per year. One third of 355 different known plant species in Kazdagi have medicinal and aromatic values, and over 50 of them are endemic species. As a pilot genetic diversity conservation site, Kazdagi has been supported by number of local, national, and international projects including a World Bank GEF project. This paper represents the first reports on the natural radionuclides in forest sites of Mount IDA/Kazdagi. Based on 118 soil profiles (341 collected soil samples), ^{40}K activity concentrations averaged over the depth sections varied within the limits from 43 to 1,008 Bq kg^{-1} with a mean of 516 Bq kg^{-1}, while the ranges of ^{226}Ra and ^{232}Th concentrations were 5–152 Bq kg^{-1} with a geometric mean of 33 and 6–275 Bq kg^{-1} with a geometric mean of 45 Bq kg^{-1}, respectively. The observed mean concentrations indicate that the radioactivity values in the forested areas at the Mount IDA (Kazdagi)/Edremit were within the universal typical ranges. The corresponding dose rates, the average effective dose equivalent, and other radiological parameters such as radium equivalent activity (Ra_{eq}), external hazard index (H_{ex}), and gamma index ($I\gamma$) were less than their respective limiting values. Thus, we found that radionuclide activity levels do not pose any significant radiological hazard for human health.

As spatial maps can provide significant information on pollution sources of radionuclides, the regional background levels for ^{40}K, ^{226}Ra, and ^{232}Th are mapped as a reference data. The radiological mapping data for the region indicate that the distributions of the ^{232}Th, ^{226}Ra, and ^{40}K activities and gamma dose rate as well show a high variation. The significant variation among ^{232}Th, ^{226}Ra, and ^{40}K activities and gamma dose rate might be due to the geological variation throughout the sampling sites. To our knowledge, this study is the first extensive investigation on representing the spatial distribution of natural radionuclide activity concentrations in litter (newly fallen needles/leaves), fermentation, and humus layers (partly and totally decomposed material) and mineral layers, separately. These experimental measurements can be used for future studies for further radiation impact assessments in forest sites.

Acknowledgments We are very grateful to Turkish Scientific and Technical Research Council (TUBİTAK; Project no: 109Y336) for providing financial support for this study. We thank Prof. Dr. Günseli Yaprak for the invaluable advice on the gamma spectroscopy; to Mr. Hüseyin Atay, Ms. Rukiye Çakır, Mr. Fatih Çoban, Mr. Emir Büyükok, and Ms. Sabiha Vurmaz for their assistance with soil sample collection and preparation of soils; and to Mr. Niyazi Özçankaya for his careful assistance in preparation of forest vegetation map of Kazdagi. We also thank Dr. Alper Akgül for his assistance in the preparation of this manuscript.

References

Al-Jundi, J. (2002). Population doses from terrestrial gamma exposure in areas near to old phosphate mine, Russaifa. Jordan. *Radiation Measurements, 35*, 23–28.

Alnour, I. A., Wagiran, H., Ibrahim, N., Laili, Z., Omar, M., Hamzah, S., & Idi, B. Y. (2012). Natural radioactivity measurements in the granite rock of quarry sites, Johor, Malaysia. *Radiation Physics and Chemistry, 81*, 1842–1847.

Altan, G., & Türkeş, M. (2011). Hydroclimatologic characteristics of the forest fires occurred at the Çanakkale district and relationship with climate variations. *Ege Coğrafya Dergisi, 20*(2), 1–25.

Anonymous (2002). Kazdagi Milli Park Müdürlügü Kayitlari, Edremit.

Aslani, M. A. A., Aytas, S., Akyil, S., Yaprak, G., Yener, G., & Eral, M. (2003). Activity concentration of Caesium-137 in agricultural soils. *Journal of Environmental Radioactivity, 65*, 131–145.

Beck, H.L. (1972) The physics of environmental gamma radiation fields. Natural Radiation Environment II, Cohewan, Canada. CONF-720805 P2. In *Proceedings of the second international symposium on the natural radiation environment* (pp 101–133).

Beretka, J., & Mathew, P. J. (1985). Natural radioactivity of Australian building materials, industrial wastes and by-products. *Health Physics, 48*, 87–95.

Canbaz, B., Çam, F., Yaprak, G., & Candan, O. (2010). Natural radioactivity (^{226}Ra, ^{232}Th and ^{40}K) and assessment of radiological hazards in the Kestanbol Granitoid, Turkey. *Radiation Protection Dosimetry, 141*(2), 192–198.

Chiozzi, P., Pasquale, V., & Verdoya, M. (2002). Naturally occurring radioactivity at the Alps-Apennines transition. *Radiation Measurument, 35*, 147–154.

Clark, S. P., Peterman, Z. K., Heider, K. S. (1966) Abundances of uranium, thorium and potassium. In: Clark SP (ed) Handbook of physical constants. *Geology Society of America Memoirs 47*, 521–541.

Currie, L. A. (1968). Limits for qualitative detection and quantitative determination. *Analytical Chemistry, 40*(3), 586–593.

Duru, M., Pehlivan, Ş., Ilgar, A., Dönmez, M., & Akçay, A. E. (2007a). *1:100 000 ölçekli Türkiye jeoloji haritaları. Balıkesir-İ18 paftası. No: 97*. Ankara: Maden Tetkik ve Arama Genel Müdürlüğü Jeoloji Etütleri Dairesi.

Duru, M., Pehlivan, Ş., Ilgar, A., Dönmez, M., & Akçay, A. E. (2007b). *1:100 000 ölçekli Türkiye jeoloji haritaları. Ayvalık-İ17 paftası. No: 98*. Ankara: Maden Tetkik ve Arama Genel Müdürlüğü Jeoloji Etütleri Dairesi.

EC (European Commission) (1999). *Radiation protection 112. Radiological protection principles concerning the Natural Radioactivity of Building Materials Directorate-General Environment*, Nuclear Safety and Civil Protection.

Fujiyoshi, R., & Sawamura, S. (2004). Mesoscale variability of vertical profiles of environmental radionuclides (^{40}K, ^{226}Ra, ^{210}Pb and ^{137}Cs) in temperate forest soils in Germany. *Science of the Total Environment, 320*, 177–188.

Gaso, M. I., Segovia, N., Morton, O., Cervantes, M. L., Godinez, L., Pena, P., & Acosta, E. (2000). ^{137}Cs and relationships with major and trace elements in edible mushrooms from Mexico. *Science of the Total Environment, 262*, 73–89.

Hejl, A. M., Ottmar, R. D., Jannik, G. T., Eddy, T. P., Rathbun, S. L., Commodore, A. A., Pearce, J. L., & Naeher, L. P. (2013). Radionuclide activity concentrations in forest surface fuels at the Savannah River Site. *Journal of Environmental Management, 115*, 217–226.

Karadeniz, Ö., & Akal, C. (2014). Radiological mapping in the granodiorite area of Bergama (Pergamon)-Kozak, Turkey. *Journal of Radioanalytical and Nuclear Chemistry, 302*, 361–373.

Karadeniz, Ö., & Yaprak, G. (2007). Distribution of radiocesium and natural gamma emitters in pine needles in coniferious forest sites of Izmir. *Applied Radiation and Isotopes, 65*(12), 1363–1367.

Karadeniz, Ö., & Yaprak, G. (2008). Vertical distributions and gamma dose rates of ^{40}K, ^{232}Th, ^{238}U and ^{137}Cs in the selected forest soils in Izmir, Turkey. *Radiation Protection Dosimetry, 131*(3), 346–355.

Karadeniz, Ö., & Yaprak, G. (2011). Activity concentrations of natural radionuclides and ^{137}Cs in soils of coniferous forest sites in West Anatolia. *European Journal of Forest Research, 130*(2), 271–276.

Kelkit, A., Özel, A. E., & Demirel, O. (2005). A study of the Kazdagi (Mt. Ida) National Park: an ecological approach to the management of tourism. *International Journal of Sustainable Development & World Ecology, 12*, 1–8.

Khoshbinfar, S., & Moghaddam, M. V. (2012). Spatial variability of soil ^{137}Cs in the South Caspian region. *Environental Monitoring and Assessment, 184*, 3053–3062.

Krieger, R. (1981). Radioactivity of construction materials. *Betonwerk und Fertigteil-Technik, 47*, 468.

Mohapatra, S., Sahoo, S. K., Vinod Kumar, A., Patra, A. C., Lenka, P., Dubey, J. S., Thakur, V. K., Tripathi, R. M., & Puranik, V. D. (2013). Distribution of norm and ^{137}Cs in soils of the Visakhapatnam Region, Eastern India, and associated radiation dose. *Radiation Protection Dosimetry, 157*(1), 95–104.

Nada, A., Abd-ElMaksoud, T. M., Abu-ZeidHosnia, M., El-Nagar, T., & Awad, S. (2009). Distribution of radionuclides in soil samples from a petrified wood forest in El-Qattamia, Cairo, Egypt. *Applied Radiation and Isotopes, 67*, 643–649.

OECD. (1979). *Nuclear Energy Agency. Exposure to radiation from natural radioactivity in building materials. Report by NEA Group of Experts*. Paris: OECD.

Örgün, Y., Altınsoy, N., Şahin, S. Y., Güngör, Y., Gültekin, A. H., Karahan, G., & Karacık, Z. (2007). Natural and

anthropogenic radionuclides in rocks and beach sands from Ezine region (Çanakkale), Western Anatolia, Turkey. *Applied Radiation and Isotopes, 65*, 739–747.

Özel, N. (1999). *Phytosociologic and phytoecologic studies on forest vegetation in Kazdaglari*. Izmir: Ege Forestry Research Institute Technical Bulletin. No: 11.

Öztürk, B. C., Çam, N. F., & Yaprak, G. (2013). Reference levels of natural radioactivity and ^{137}Cs in and around the surface soils of Kestanbol pluton in Ezine region of Çanakkale province, Turkey. *Journal of Environmental Science and Health, Part A, 48*, 1522–1532.

Ramli, A. T. (1997). Environmental terrestrial gamma radiation dose and its relationship with soil type and underlying geological formations in Pontian District, Malaysia. *Applied Radiation and Isotopes, 48*(3), 407–412.

Rühm, W., Yoshida, S., Muramatsu, Y., Steiner, M., & Wirth, E. (1999). Distribution patterns for stable ^{133}Cs and their implications with respect to the long-term fate of radioactive ^{134}Cs and ^{137}Cs in a semi-natural ecosystem. *Journal of Environmental Radioactivity, 45*, 253–270.

Segovia, N., Gaso, M. I., Alvarado, E., Pena, P., Morton, O., Armienta, M. A., & Reyes, A. V. (2003). Environmental radioactivity studies in the soil of a coniferous forest. *Radiation Measurement, 36*, 525–528.

Soil Survey Staff. (2014). *Keys to soil taxonomy* (12th ed.). Washington, DC: USDA—Natural Resources Conservation Service.

Tufail, M., Akhtar, N., & Waqas, M. (2006). Measurement of terrestrial radiation for assessment of gamma dose from cultivated and barren saline soils of Faisalabad in Pakistan. *Radiation Measurements, 41*, 443–451.

Tzortzis, M., & Tsertos, H. (2004). Determination of thorium, uranium and potassium elemental concentrations in surface soils in Cyprus. *Journal of Environmental Radioactivity, 77*, 325–338.

Tzortzis, M., Tsertosa, H., Christofides, S., & Christodoulides, G. (2003). Gamma-ray measurements ofnaturally occurring radioactive samples from Cyprus characteristic geological rocks. *Radiation Measurements, 37*, 221–229.

UNSCEAR (1982). *Sources and biological effects of ionizing radiation*. Report to General Assembly, with Scientific Annexes, United Nations, New York.

UNSCEAR (2000). *Sources and biological effects of ionizing radiation*. Report to General Assembly, with Scientific Annexes, United Nations, New York.

Uysal, I. (2010). An overview of plant diversity of Kazdagi (Mt. Ida) Forest National Park, Turkey. *Journal of Environmental Biology, 31*, 141–147.

Vaca, F., Manjon, G., & Garcia-Leon, M. (2001). The presence of some artificial and natural radionuclides in a Eucalyptus forest in the South of Spain. *Journal of Environmental Radioactivity, 56*, 309–325.

Verdoya, M., Chiozzi, P., & Pasquale, V. (2001). Heat-producing radionuclides in metamorphic rocks of the Brianconnais-Piedmont Zone (Maritime Alps). *Eclogae Geologicae Helvetiae, 94*, 1–7.

Yaprak, G., & Aslani, M. A. A. (2010). External dose-rates for natural gamma emitters in soils from an agricultural land in West Anatolia. *Journal of Radioanalytical and Nuclear Chemistry, 283*(2), 279–287.

Ylipieti, J., Rissanen, K., Kostiainen, E., Salminen, R., Tomilina, O., Täht, K., Gilucis, A., & Gregorauskiene, V. (2008). Chernobyl fallout in the uppermost (0–3 cm) humus layer of forest soil in Finland, North East Russia and the Baltic countries in 2000–2003. *Science of the Total Environment, 407*, 315–323.

Zhiyanski, M., Bech, J., Sokolovska, M., Lucot, E., Bech, J., & Badot, P. M. (2008). Cs-137 distribution in forest floor and surface soil layers from two mountainous regions in Bulgaria. *Journal of Geochemical Exploration, 96*, 256–266.